Unveiling Microscopic Structures of Charged Water Interfaces by Surface-Specific Vibrational Spectroscopy

Yu-Chieh Wen,[1,2,3] Shuai Zha,[1] Xing Liu,[4,5] Shanshan Yang,[1] Pan Guo,[4,5] Guosheng Shi,[4] Haiping Fang,[4] Y. Ron Shen,[1,2,*] and Chuanshan Tian[1,6,†]

[1]*Department of Physics, State Key Laboratory of Surface Physics, and Key Laboratory of Micro- and Nano-Photonic Structures (MOE), Fudan University, Shanghai 200433, People's Republic of China*

[2]*Department of Physics, University of California, Berkeley, California 94720, USA*

[3]*Institute of Physics, Academia Sinica, Taipei 11529, Taiwan, Republic of China*

[4]*Division of Interfacial Water and Key Laboratory of Interfacial Physics and Technology, Shanghai Institute of Applied Physics, Chinese Academy of Sciences, Shanghai 201800, People's Republic of China*

[5]*University of Chinese Academy of Sciences, Beijing 100049, People's Republic of China*

[6]*Collaborative Innovation Center of Advanced Microstructures, Fudan University, Shanghai 200433, People's Republic of China*

(Received 26 September 2015; published 5 January 2016)

A sum-frequency spectroscopy scheme is developed that allows the measurement of vibrational spectra of the interfacial molecular structure of charged water interfaces. The application of this scheme to a prototype lipid-aqueous interface as a demonstration reveals an interfacial hydrogen-bonding water layer structure that responds sensitively to the charge state of the lipid headgroup and its interaction with specific ions. This novel technique provides unique opportunities to search for better understanding of electrochemistry and biological aqueous interfaces at a deeper molecular level.

DOI: 10.1103/PhysRevLett.116.016101

Knowing the molecular structure of water next to a charged substrate is a prerequisite to the fundamental understanding of many natural phenomena and is of great importance in the development of advanced energy-conversion and storage devices. Protein folding [1,2], photocatalysis for water splitting [3–5], and proton-exchange membrane fuel cells [6] are just a few familiar examples. At these interfaces, water molecules, solvated ions, and the charged substrate interact strongly with one another through hydrogen (H) bonding, electrostatic force, and van der Waals force within a distance of a few monolayers away from the surface, forming an interface-specific bonding network [7,8]. It has been long recognized that this interfacial region, labeled here as "the bonded interface layer (BIL)," is mainly responsible for electrochemistry at interfaces and directly controls many elementary processes, such as ion desolvation and charge transfer in chemical reactions [2–4,9]. Next to the BIL, the deeper water subphase has essentially the bulk H-bonding structure that could be influenced by a long-range dc field set up by surface charges and the screening ions in a region known as the diffuse layer [10–13].

Despite the importance of the BIL, current knowledge on its microscopic structure and the interplay between ionic and molecular species therein is very limited [7,8,11–21]. The difficulty lies in the paucity of experimental techniques that allow the extraction of structural information about such a layer in the presence of a diffuse layer [8,11–21]. Infrared spectroscopy cannot distinguish spectral contributions from the two layers [21]. Scanning tunneling microscopy and atomic force microscopy probe the local structure of an interface, but the measurement is strongly perturbed by the dynamic movements of aqueous molecules [7]. X-ray adsorption spectroscopy was recently employed to study populations of donor-H-bond water species at an electrode-water interface [8], but the result does not yield information on the geometry of the interfacial structure. Optical second-harmonic generation [20] and sum-frequency generation (SFG) [11–19] are forbidden in media with inversion symmetry but necessarily allowed at interfaces. They have been widely used to investigate aqueous interfaces. At a charged water interface, a sum-frequency (SF) spectrum has contributions from both the noncentrosymmetric BIL and the diffuse layer with inversion symmetry broken by the surface field, but the experimental separation of the two contributions is difficult. In many reports, the attention was on the diffuse layer; the contribution from the BIL was simply ignored [11–13]. In others, the interpretation of the results is vague and questionable [14–16]. In a recent paper, Jena *et al.* [17] attempted to interpret a set of SF intensity spectra of water-silica interfaces with different NaCl concentrations in water in terms of the contributions from water in the BIL and the diffuse layer. No separate spectral information on the BIL and the diffuse layer could be retrieved.

In this Letter, we report the development of a phase-sensitive sum-frequency vibrational spectroscopy (PS-SFVS) scheme that allows the deduction of vibrational spectra and, hence, microscopic structural information of the BIL of charged water interfaces. The scheme is based on the idea that the SF vibrational spectrum of water in the diffuse layer (DL), $\chi^{(2)}_{S,\mathrm{DL}}(\omega)$, can be found if the dc field distribution E_0 in the DL and the dc-field-induced SF

response of the bulk water are known. With $\chi^{(2)}_{S,\mathrm{DL}}(\omega)$ available, the spectrum of the BIL, $\chi^{(2)}_{S}(\omega)$, can be readily extracted from the measured effective surface nonlinear susceptibility $\chi^{(2)}_{S,\mathrm{eff}}(\omega)$, as we shall explain later. The application of this method to a prototype lipid-water interface reveals significant variation of its BIL structure upon deprotonation of the lipid headgroups and the interaction of specific ions with the headgroups. This spectroscopic technique offers a viable means for *in situ* probing of electrochemical and aqueous biological interfaces at the molecular level.

Our model of a charged water interface is based on the double-layer theory [10] with particular concern about the molecular structure. As sketched in Fig. 1(a), we consider an interface between water and a semi-infinite isotropic medium at $z = 0$ (with z along the surface normal). The BIL ($0 < z < 0^+$) is expected to be very thin because it is known that the surface-induced H-bonding structural change should relax away in a few monolayers [22]. It is followed by bulklike water in the diffuse layer ($z > 0^+$) that has an effective thickness defined by the Debye length λ_D [10] and is under the influence of the dc field $\hat{z}E_0(z)$. The exact position of 0^+ is not important for the analysis. The reflected SFG from the interfacial system has its field proportional to the effective surface nonlinear polarization $\mathbf{P}^{(2)}_S$ at the sum frequency $\omega_{\mathrm{SF}}(=\omega_{\mathrm{VIS}}+\omega)$, given by $\mathbf{P}^{(2)}_S(\omega_{\mathrm{SF}}) = \chi^{(2)}_{S,\mathrm{eff}}\colon \mathbf{E}(\omega_{\mathrm{VIS}})\mathbf{E}(\omega)$ [23]. It has been repeatedly shown that $\chi^{(2)}_{S,\mathrm{eff}}$ contains both surface and bulk contributions [23,24]. A simple derivation yields

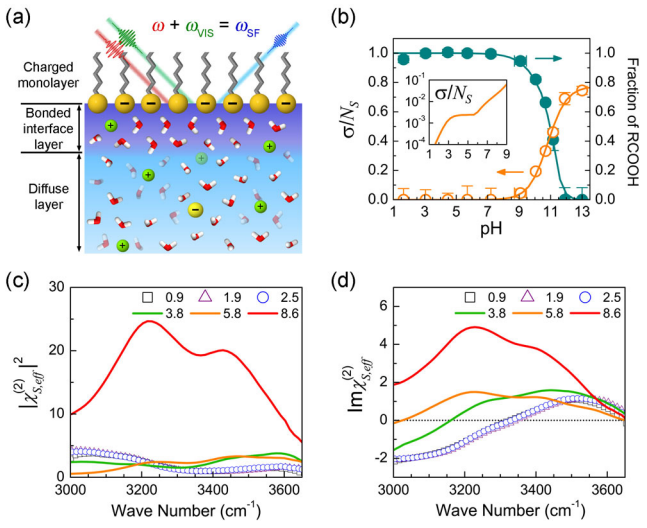

FIG. 1. (a) Illustration of a charged interfacial structure probed by SFVS. (b) Fractional surface densities of unionized COOH and negative charges σ/N_S of the lignoceric acid monolayer on water versus pH (dots), where N_S is the surface density of the monolayer. Lines are guides for the eyes. The inset shows the calculated σ/N_S in the low-pH range. (c),(d) OH stretching spectra of $|\chi^{(2)}_{S,\mathrm{eff}}|^2$ and $\mathrm{Im}\chi^{(2)}_{S,\mathrm{eff}}$ for the lignoceric acid monolayer-water interface at various pH, respectively.

$$\chi^{(2)}_{S,\mathrm{eff}} = \chi^{(2)}_{S} + \int_{0^+}^{\infty} [\chi^{(2)}_{B} + \chi^{(3)}_{B}\cdot\hat{z}E_0(z')]e^{i\Delta k_z z'}dz', \quad (1)$$

with $\chi^{(2)}_B$ and $\chi^{(3)}_B$ denoting the second-order electric-quadrupole bulk nonlinear susceptibility and the third-order bulk nonlinear susceptibility of water, respectively, independent of interfaces, and $\Delta k_z = k_{\mathrm{SF},z} + k_{\mathrm{VIS},z} + k_z$ describing the phase mismatch of the reflected SFG. We have used linear approximation to describe the dc-field-induced SF nonlinearity, $\chi^{(3)}_B(z)\cdot\hat{z}E_0(z)$, at z. Generally, $\chi^{(3)}_B$ is dominated by field-induced reorientation of water molecules, although it can also have contribution from field-induced changes of the H-bonding structure and electron polarizabilities of the molecules [12,20,24]. For the SFVS of water with S-, S-, and P-polarized SF, visible, and IR fields, it has been found that the $\chi^{(2)}_B$ term in Eq. (1) is negligible [25]. We then have

$$\chi^{(2)}_{S,\mathrm{eff}} = \chi^{(2)}_{S} + \chi^{(2)}_{S,\mathrm{DL}},$$
$$\chi^{(2)}_{S,\mathrm{DL}} \equiv \int_{0^+}^{\infty} \chi^{(3)}_B\cdot\hat{z}E_0(z')e^{i\Delta k_z z'}dz' \equiv \chi^{(3)}_B\cdot\hat{z}\Psi,$$
$$\text{with}\quad \Psi \equiv \int_{0^+}^{\infty} E_0(z')e^{i\Delta k_z z'}dz'. \quad (2)$$

We note that both $\chi^{(2)}_S$ and $\chi^{(2)}_{S,\mathrm{DL}}$ act as surface nonlinear susceptibilities, but it is $\chi^{(2)}_S$ of the BIL that is of interest to us [26].

In order to extract $\chi^{(2)}_S(\omega)$ from the measured $\chi^{(2)}_{S,\mathrm{eff}}(\omega)$, we need to know $\chi^{(3)}_B(\omega)$ and $E_0(z)$. If the surface charge density σ is less than a few percent of a monolayer, the spectral change of the BIL due to the structural perturbation is hardly detectable [14], so that $\chi^{(2)}_S(\omega)$ is essentially the same as that of the neutral interface, denoted by $\chi^{(2)}_{S0}(\omega)$, but the dc-field-induced $\chi^{(2)}_{S,\mathrm{DL}}(\omega)$ of the diffuse layer could be significant [14]. Therefore, for low σ, we can obtain $\chi^{(2)}_{S,\mathrm{DL}}(\omega)$ simply from the difference of measured $[\chi^{(2)}_{S,\mathrm{eff}}(\omega)]_{\sigma}$ and $[\chi^{(2)}_{S,\mathrm{eff}}(\omega)]_{\sigma=0} = \chi^{(2)}_{S0}(\omega)$. With the help of the Gouy-Chapman (GC) theory, we can find $E_0(z)$ for a given σ and then deduce the spectrum of $\chi^{(3)}_B(\omega)$ from $\chi^{(2)}_{S,\mathrm{DL}}(\omega)$ following Eq. (2). With $\chi^{(3)}_B(\omega)$ known and $E_0(z)$ calculated from the GC or a more refined theory [10], we can then obtain $\chi^{(2)}_{S,\mathrm{DL}}(\omega)$ for any charged water interface with given σ from Eq. (2), and, subsequently, $\chi^{(2)}_S(\omega)$ can be deduced from the difference of the measured $\chi^{(2)}_{S,\mathrm{eff}}(\omega)$ and the calculated $\chi^{(2)}_{S,\mathrm{DL}}(\omega)$.

In our experiment, the sample was a monolayer of lignoceric acid ($C_{23}H_{47}COOH$) on water probed by a broadband PS-SFVS setup (see the Supplemental Material [27]). The pH of water was varied by adjusting

the concentration of HCl or NaOH in water. How the charge state of the monolayer varies with pH was studied earlier [18,19]; it was determined from the CO stretch modes of the fatty acid headgroups, including COOH, COO^-, and $COO^- \cdots Na^+$ complex, in the SF spectrum. (See the Supplemental Material [27] Sec. S2 for details.) Shown in Fig. 1(b) are the surface densities of COOH and (negative) σ resulting from COO^- and $COO^- \cdots Na^+$ vs pH deduced from our SFVS measurement [27]. It is seen that the interface is neutral at low pH and increasingly charged with pH upon deprotonation of the monolayer. At pH 9, the fractional ionization of the headgroups is still only ~5% but rapidly increases to full deprotonation at $p\mathrm{H} \sim 12$. The surface charge density σ does not change proportionally due to the appearance of $COO^- \cdots Na^+$ at $p\mathrm{H} > 10.5$. For $p\mathrm{H} < 9$, the spectral feature of COO^- was too weak to allow deduction of σ, and we relied on the deprotonation reaction equation for fatty acid and the GC theory to find σ (see the Supplemental Material [27] Sec. S2 for details), which is displayed in the inset of Fig. 1(b).

The measured $|\chi^{(2)}_{S,\mathrm{eff}}|^2$ and $\mathrm{Im}\chi^{(2)}_{S,\mathrm{eff}}$ spectra in the OH stretching range for the fatty acid monolayer on water at different pH are presented in Figs. 1(c) and 1(d). At pH below 2.5, $\chi^{(2)}_{S,\mathrm{eff}}$ remains unchanged, showing that the interface is essentially neutral with $\chi^{(2)}_{S,\mathrm{eff}}(\omega) \cong \chi^{(2)}_{S0}(\omega)$. For $2.5 < p\mathrm{H} < 9$, the observed $\chi^{(2)}_{S,\mathrm{eff}}(\omega)$ varies, but we still expect $\chi^{(2)}_{S}(\omega) \cong \chi^{(2)}_{S0}(\omega)$ for low σ. From the difference between $\chi^{(2)}_{S,\mathrm{eff}}(\omega)$ and $\chi^{(2)}_{S0}(\omega)$, we can then obtain $\chi^{(2)}_{S,\mathrm{DL}}(\omega)$ depicted in Fig. 2(a), which depends on pH through $E_0(z)$ according to Eq. (2). At a given pH in this range, we can use the GC theory with the known $\mathrm{pK}_a(\sim 5.6)$ [27,43] for deprotonation of fatty acid to find σ and Ψ shown in the Supplemental Material [27] Fig. S3. Following Eq. (2), we

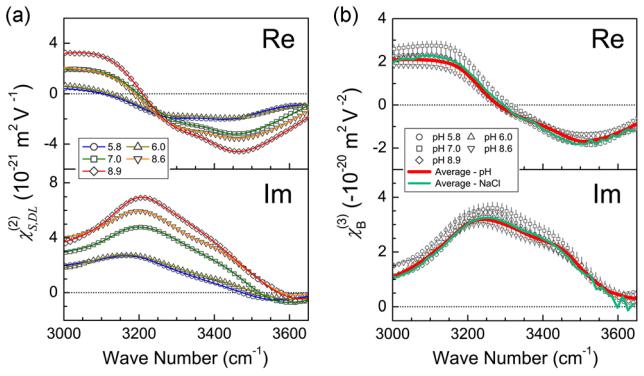

FIG. 2. (a) Spectra of complex $\chi^{(2)}_{S,\mathrm{DL}}$ of the diffuse layer and (b) spectra of complex $\chi^{(3)}_B$ of bulk water in the OH stretching region at various pH deduced from the spectra of lignoceric acid monolayer-water interfaces in Figs. 1(c) and 1(d). The red curve in (b) for $\chi^{(3)}_B(\omega)$ is a weighted average of the spectra for different pH. The green curve is an average of $\chi^{(3)}_B(\omega)$ obtained from a set of $\chi^{(2)}_{S,\mathrm{eff}}(\omega)$ spectra presented in Fig. S9 of the Supplemental Material [27], taken at pH 6 with different NaCl concentrations in water.

can then deduce $\chi^{(3)}_B(\omega)$ from $\chi^{(2)}_{S,\mathrm{DL}}(\omega)$ and Ψ. We expect that if the analysis is correct, the deduced $\chi^{(3)}_B(\omega)$ being characteristic of the bulk water should be independent of pH. This is indeed what we found, as shown in Fig. 2(b). The result also indicates that the GC theory is valid in this pH range. To further confirm our scheme, we measured $\chi^{(2)}_{S,\mathrm{eff}}(\omega)$ of the same interfacial system at pH 6 for a number of NaCl concentrations in the solution. The spectra of $\chi^{(2)}_{S,\mathrm{eff}}(\omega)$ displayed in the Supplemental Material [27] Fig. S9 are obviously different for different NaCl concentrations. Again, with $\chi^{(2)}_{S}(\omega) \cong \chi^{(2)}_{S0}(\omega)$, we can obtain $\chi^{(2)}_{S,\mathrm{DL}}(\omega)$ from $\chi^{(2)}_{S,\mathrm{eff}}(\omega)$, and following the GC theory and Eq. (2), we find $\chi^{(3)}_B(\omega)$, which is plotted in Fig. 2(b) in comparison with those deduced earlier. The agreement is well within the experimental accuracy.

At high pH (> 9), the fraction of deprotonation becomes increasingly significant, and the structure of the BIL changes accordingly so that the $\chi^{(2)}_{S}(\omega)$ spectrum is expected to also vary with the pH. In this case, the simple GC theory may break down because at high ionic concentrations, the size of ions can no longer be neglected. Instead, a modified GC theory (described in the Supplemental Material [27] Sec. S4) that takes into account the steric effect of ions must be employed [44,45]. Shown in the Supplemental Material [27] Fig. S4 is a comparison of σ deduced from the measured spectra in the CO stretching range with those calculated from the simple and modified GC models. While the simple GC theory appears to appreciably overestimate σ for $p\mathrm{H} > 9$, the modified GC theory with an effective ion size of ~7 Å, which is close to the values adopted by others [44,45], fits the measured σ versus pH well.

We can now use the modified GC theory and Eq. (2) to obtain $\chi^{(2)}_{S,\mathrm{DL}}(\omega)$ from the previously deduced $\chi^{(3)}_B(\omega)$ for any given pH or σ, and extract $\chi^{(2)}_{S}(\omega)$ from the difference between $\chi^{(2)}_{S,\mathrm{DL}}(\omega)$ and the measured $\chi^{(2)}_{S,\mathrm{eff}}(\omega)$. The $\mathrm{Im}\chi^{(2)}_{S}(\omega)$ spectra so obtained for pH 10.6 and 12 are presented in Fig. 3(a) in comparison with that of the neutral interface (see the Supplemental Material [27] Fig. S10 for a detailed analysis). The $\mathrm{Im}\chi^{(2)}_{S}(\omega)$ spectra are obviously different, reflecting significantly different structures of the BIL. A brief discussion of the spectra is in order here, but the details will appear elsewhere. The $\mathrm{Im}\chi^{(2)}_{S0}(\omega)$ spectrum for the neutral interface (pH 2.5) has a negative OH stretching band below 3350 cm^{-1} extending beyond 3000 cm^{-1}. It comes mainly from down-pointing OH of COOH of the fatty acid headgroups and partly from down-pointing OH of water molecules with O acceptor bonded to H of COOH. The positive band from 3350 to 3650 cm^{-1} is dominated by up-pointing OH of water molecules weakly donor bonded to O of COOH. With increasing pH, $\mathrm{Im}\chi^{(2)}_{S}(\omega)$ exhibits significant variation, revealing a structural change of the

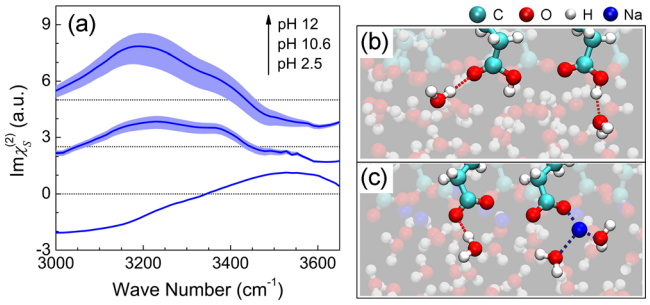

FIG. 3. (a) OH stretching spectra of the BIL of the lignoceric acid monolayer-water interface at three pH values with different interface charging conditions: pH 2.5, 10.6, and 12 corresponding to the fractional density of COO^- $(\mathrm{COO}^- \cdots \mathrm{Na}^+) = 0\%$ (0%), 27% (9%), and 39% (52%) of the monolayer, respectively. The shadowed regions denote uncertainty, and the spectra are vertically shifted for clarity. (b),(c) Side-view snapshots of the MD trajectories for the neutral and fully deprotonated fatty acid–water interfaces, respectively. Major bonding configurations at the interfaces are emphasized in opaque. Detailed MD results are given in Ref. [27].

BIL in response to deprotonation and specific cation interaction with the fatty acid headgroups. The nearly fully deprotonated monolayer ($p\mathrm{H} \sim 12$) is composed of COO^- and $\mathrm{COO}^- \cdots \mathrm{Na}^+$. The spectrum displays a broad positive band from 3000 to 3450 cm^{-1}, which must be dominated by up-pointing OH of water molecules donor bonded to O of COO^-. The negative band at higher frequency may arise from water molecules associated with Na^+. Hydrated Na^+ ions in bulk water are expected to have their associated water molecules symmetrically distributed around them with O facing the ions. The association of Na^+ with surface COO^- breaks the up-down symmetry and results in more surrounding water molecules with OH pointing downward. There could also be contribution from down-pointing OH of water molecules that have the other OH donor bonded to the fatty acid headgroups.

We have carried out molecular dynamics (MD) simulations on the neutral and fully deprotonated fatty acid–water interfaces at 300 K (see the Supplemental Material [27] Sec. S5 for details). The analysis of the MD trajectories provides information about populations of different bonding configurations between water molecules and the headgroups of the fatty acid monolayer and the orientation distributions of the donor-bonded OH. The results show that the H-bonding structure of the water molecules responds sensitively to the charge state of the fatty acid headgroups (see the Supplemental Material [27] Figs. S7 and S8). They are in qualitative agreement with the aforementioned interfacial structures constructed from the experiment.

To further confirm the general applicability of our scheme, we carried out another experiment using a different interfacial system. One would expect that $\chi_B^{(3)}(\omega)$ should be independent of the interfacial system chosen. The system we chose here was an octadecanol (R'OH) monolayer doped by $f\%$ of lignoceric acid covering a 0.1 mM NaCl solution. With small amount of doping ($f < 5$), the BIL structure is dictated by the charge-neutral alcohol molecules, and $\mathrm{Im}\chi_S^{(2)}(\omega)$ for $f < 5$ is essentially the same as that of a pure octadecanol monolayer on water. Figure 4 shows a set of $\mathrm{Im}\chi_{S,\mathrm{eff}}^{(2)}$ spectra taken with different f and the $\mathrm{Im}\chi_B^{(3)}(\omega)$ spectrum deduced from them using Eq. (2) and the GC theory. The $\mathrm{Im}\chi_S^{(2)}(\omega)$ spectrum measured at $f = 0$ is quite different from that of the neutral fatty acid monolayer in Fig. 3(a), indicating distinctly different structures of the two neutral interfaces. On the other hand, the deduced $\mathrm{Im}\chi_B^{(3)}(\omega)$ is, as expected, consistent with that obtained from the fatty acid case within experimental error [Fig. 4(b)]. As a bulk spectrum, $\mathrm{Im}\chi_B^{(3)}(\omega)$ shows a characteristic broad OH stretching band with two humps at ~3220 and ~3450 cm^{-1} that are also present in IR and Raman spectra of bulk water [46]. However, the relative spectral weight of the two humps does not resemble that of the IR or Raman spectrum. This is likely due to strong dynamic coupling between neighboring water molecules that strengthens the lower-frequency OH stretch band, as pointed out by Morita, Skinner, and co-workers [22,46,47].

We have demonstrated a scheme using PS-SFVS to separately deduce the vibrational spectra of the BIL and the diffuse layer of a charged water interface. For any water interface with a given surface charge density σ, it is now possible to find the spectrum of the diffuse layer and, in turn, the spectrum of the BIL from measurement. Even if σ is not known, one can still carry out a measurement with several different phase mismatches Δk_z, and deduce both σ and the spectrum of the BIL, which are intimately related to the microscopic structure of BIL. Such work offers new

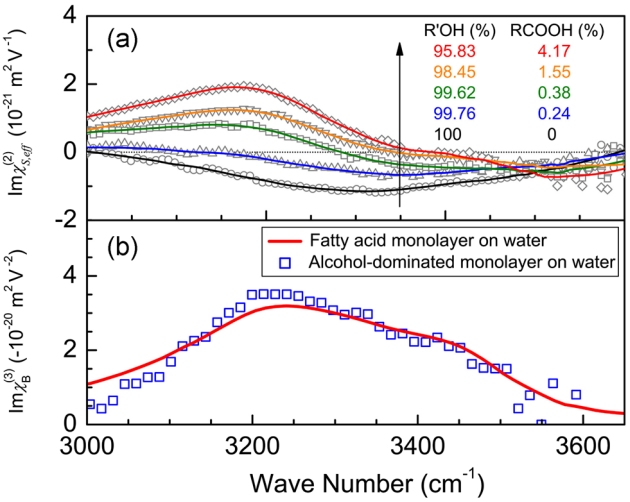

FIG. 4. (a) Measured OH stretching spectra of $\mathrm{Im}\chi_{S,\mathrm{eff}}^{(2)}$ of an octadecanol monolayer mixed with small fractions of lignoceric acid on 0.1 mM NaCl solution (dots). Lines are guides to the eyes. (b) Weighted average of $\mathrm{Im}\chi_B^{(3)}(\omega)$ deduced from $\mathrm{Im}\chi_{S,\mathrm{eff}}^{(2)}(\omega)$ in (a) in comparison with the average $\mathrm{Im}\chi_B^{(3)}$ spectrum (red curve) given in Fig. 2(b).

opportunities to explore various charged water interfaces at a deeper molecular level, providing a base for the understanding and theoretical modeling of such interfaces.

The authors thank Dr. Yimin Li and Dr. Zhi Liu for helpful discussion. Y. C. W. thanks Academia Sinica for supporting this study. C. S. T. acknowledges support by the NSFC (Grants No. 11374064, No. 11290161, and No. 11104034) and NCET Grant No. 130141. H. P. F. acknowledges support from the NSFC (Grant No. 11290164). Y. R. S. acknowledges support from the Director of the Office of Science, Office of Basic Energy Sciences, Materials Sciences and Engineering Division of the U.S. Department of Energy under Contract No. DE-AC03-76SF00098.

*Corresponding author.
yrshen@berkeley.edu
†Corresponding author.
cstian@fudan.edu.cn

[1] L. Y. Zhang, Y. Yang, Y. T. Kao, L. J. Wang, and D. P. Zhong, J. Am. Chem. Soc. **131**, 10677 (2009).
[2] P. Lo Nostro and B. W. Ninham, Chem. Rev. **112**, 2286 (2012).
[3] G. A. Sormorjai, *Introduction to Surface Chemistry and Catalysis* (Wiley, New York, 1994).
[4] G. E. Brown *et al.*, Chem. Rev. **99**, 77 (1999).
[5] R. Asahi, T. Morikawa, T. Ohwaki, K. Aoki, and Y. Taga, Science **293**, 269 (2001).
[6] H. Liu and B. E. Logan, Environ. Sci. Technol. **38**, 4040 (2004).
[7] P. Allongue, Phys. Rev. Lett. **77**, 1986 (1996).
[8] J.-J. Velasco-Velez, C. H. Wu, T. A. Pascal, L. F. Wan, J. Guo, D. Prendergast, and M. Salmeron, Science **346**, 831 (2014).
[9] The BIL is analogous to the Helmholtz layer in the double-layer theory for ions from the aspect of their spatial distribution.
[10] A. J. Bard and L. R. Faulkner, *Electrochemical Methods: Fundamentals and Applications* (Wiley, New York, 1980).
[11] D. Lis, E. H. G. Backus, J. Hunger, S. H. Parekh, and M. Bonn, Science **344**, 1138 (2014).
[12] D. E. Gragson, B. M. McCarty, and G. L. Richmond, J. Am. Chem. Soc. **119**, 6144 (1997).
[13] S. Nihonyanagi, S. Yamaguchi, and T. Tahara, J. Am. Chem. Soc. **136**, 6155 (2014).
[14] C. S. Tian and Y. R. Shen, Proc. Natl. Acad. Sci. U.S.A. **106**, 15148 (2009).
[15] J. A. Mondal, S. Nihonyanagi, S. Yamaguchi, and T. Tahara, J. Am. Chem. Soc. **134**, 7842 (2012).
[16] V. Ostroverkhov, G. A. Waychunas, and Y. R. Shen, Phys. Rev. Lett. **94**, 046102 (2005).
[17] K. C. Jena, P. A. Covert, and D. K. Hore, J. Phys. Chem. Lett. **2**, 1056 (2011).
[18] P. B. Miranda, Q. Du, and Y. R. Shen, Chem. Phys. Lett. **286**, 1 (1998).
[19] C. Y. Tang and H. C. Allen, J. Phys. Chem. A **113**, 7383 (2009).
[20] S. W. Ong, X. L. Zhao, and K. B. Eisenthal, Chem. Phys. Lett. **191**, 327 (1992).
[21] G. Lefevre, Adv. Colloid Interface Sci. **107**, 109 (2004).
[22] T. Nagata and S. Mukamel, J. Am. Chem. Soc. **132**, 6434 (2010).
[23] Y. R. Shen, J. Phys. Chem. C **116**, 15505 (2012); **117**, 11884(E) (2013).
[24] Y. R. Shen, *The Principles of Nonlinear Optics* (Wiley, New York, 1984).
[25] X. Wei, Ph.D. thesis, University of California at Berkeley, 2000.
[26] The phase factor ($i\Delta k_z z$) is important when the bulk ionic concentration is not sufficiently high. For example, for $\Delta k_z \lambda_D > 15°$ corresponding to ionic concentration of 1.5 mM, neglecting the phase factor may lead to an appreciable distortion of a deduced spectrum using Eq. (2).
[27] See the Supplemental Material http://link.aps.org/supplemental/10.1103/PhysRevLett.116.016101, which includes Refs. [28–42], for details of experimental method and samples, spectroscopic analysis of the monolayer deprotonation, application of the GC and modified GC theories to the spectrum analysis, MD simulations and discussions, and supplementary figures.
[28] F. Leveiller, D. Jacquemain, L. Leiserowitz, K. Kjaer, and J. Alsnielsen, J. Phys. Chem. **96**, 10380 (1992).
[29] J. Pignat, J. Daillant, L. Leiserowitz, and F. Perrot, J. Phys. Chem. B **110**, 22178 (2006).
[30] I. Kuzmenko, V. M. Kaganer, and L. Leiserowitz, Langmuir **14**, 3882 (1998).
[31] M. Carrillo-Tripp, H. Saint-Martin, and I. Ortega-Blake, J. Chem. Phys. **118**, 7062 (2003).
[32] E. F. Aziz, N. Ottosson, S. Eisebitt, W. Eberhardt, B. Jagoda-Cwiklik, R. Vacha, P. Jungwirth, and B. Winter, J. Phys. Chem. B **112**, 12567 (2008).
[33] M. Nara, H. Torii, and M. Tasumi, J. Phys. Chem. **100**, 19812 (1996).
[34] S. Usui and T. W. Healy, J. Colloid Interface Sci. **250**, 371 (2002).
[35] C. Wang, H. Lu, Z. Wang, P. Xiu, B. Zhou, G. Zuo, R. Wan, J. Hu, and H. Fang, Phys. Rev. Lett. **103**, 137801 (2009).
[36] G. Shi, J. Liu, C. Wang, B. Song, Y. Tu, J. Hu, and H. Fang, Sci. Rep. **3**, 3436 (2013).
[37] C. Wang, B. Zhou, Y. Tu, M. Duan, P. Xiu, J. Li, and H. Fang, Sci. Rep. **2**, 358 (2012).
[38] P. Guo, Y. Tu, J. Yang, C. Wang, N. Sheng, and H. Fang, Phys. Rev. Lett. **115**, 186101 (2015).
[39] B. Hess, C. Kutzner, D. van der Spoel, and E. Lindahl, J. Chem. Theory Comput. **4**, 435 (2008).
[40] W. L. Jorgensen, D. S. Maxwell, and J. TiradoRives, J. Am. Chem. Soc. **118**, 11225 (1996).
[41] H. J. C. Berendsen, J. R. Grigera, and T. P. Straatsma, J. Phys. Chem. **91**, 6269 (1987).
[42] U. Essmann, L. Perera, M. L. Berkowitz, T. Darden, H. Lee, and L. G. Pedersen, J. Chem. Phys. **103**, 8577 (1995).
[43] E. Le Calvez, D. Blaudez, T. Buffeteau, and B. Desbat, Langmuir **17**, 670 (2001).
[44] I. Borukhov, D. Andelman, and H. Orland, Phys. Rev. Lett. **79**, 435 (1997).
[45] M. S. Kilic, M. Z. Bazant, and A. Ajdari, Phys. Rev. E **75**, 021502 (2007).
[46] B. M. Auer and J. L. Skinner, J. Chem. Phys. **128**, 224511 (2008).
[47] T. Ishiyama and A. Morita, Chem. Phys. Lett. **431**, 78 (2006).